Available online at www.sciencedirect.com
SCIENCE DIRECT
Polymer 47 (2006) 3557–3564
polymer
www.elsevier.com/locate/polymer

Mechanical properties, morphology, and crystallization behavior of blends of poly(L-lactide) with poly(butylene succinate-*co*-L-lactate) and poly(butylene succinate)

Mitsuhiro Shibata [a,*], Yusuke Inoue [a], Masanao Miyoshi [b]

[a] *Department of Life and Environmental Sciences, Faculty of Engineering, Chiba Institute of Technology, 2-17-1, Tsudanuma, Narashino, Chiba 275-0016, Japan*
[b] *Shiga Films Center, C.I. Kasei Co. Ltd, 3-3-1, Maruyama, Konan, Shiga 520-3185, Japan*

Received 26 August 2005; received in revised form 24 January 2006; accepted 18 March 2006

Abstract

The blends of poly(L-lactide) (PLLA) with poly(butylene succinate) (PBS) and poly(butylene succinate-*co*-L-lactate) (PBSL) containing the lactate unit of ca. 3 mol% were prepared by melt-mixing and subsequent injection molding, and their mechanical properties, morphology, and crystallization behavior have been compared. Dynamic viscoelasticity and SEM measurements of the blends revealed that the extent of the compatibility of PBSL and PBS with PLLA is almost the same, and that the PBSL and PBS components in the blends with a low content of PBSL or PBS (5–20 wt%) are homogenously dispersed as 0.1−0.4 μm particles. The tensile strength and modulus of the blends approximately followed the rule of mixtures over the whole composition range except that those of PLLA/PBS 99/1 blend were exceptionally higher than those of pure PLLA. All the blends showed considerably higher elongation at break than pure PLLA, PBSL, and PBS. Differential scanning calorimetric analysis of the blends revealed that the isothermal and non-isothermal crystallization of the PLLA component is promoted by the addition of a small amount of PBSL, while the addition of PBS was much less effective.

Keywords: Blend of poly(L-lactide); Poly(butylene succinate-*co*-lactate); Poly(butylene succinate)

1. Introduction

Biodegradable polyesters such as poly(L-lactide) (PLLA) [1], poly(butylene succinate) (PBS) [2], poly(butylene adipate/terephthalate) (PBAT) [3], poly(ethylene terephthalate/succinate) (PETS) [4], poly(ε-caprolactone) (PCL) [5], etc. have been extensively investigated, since 1970s, in order to reduce the environmental pollution caused by plastic wastes. Recently, the polymers derived from renewable resources have been gathering much attention among their polyesters from the standpoint of conserving our petrochemical resources [6,7]. Especially, PLLA, which can be prepared from starch via fermentation has been widely used to biomaterials and construction materials [8,9]. However, its brittleness [10,11] and low crystallization rate [12] are major defects for many applications. In order to improve such properties, the blends of PLLA with other flexible and biodegradable polyesters such as PBS [13,14] and PCL [15–17] have been investigated. Regarding PLLA/PBS blend, Takagi et al. reported that the cold crystallization temperature of PLLA component shifts to a lower temperature region by the addition of PBS of 20 wt%, and that elongation at break is improved by the addition of PBS more than 60 wt% [13]. Recently, as a new type of PBS-based biodegradable polyester, poly(butylene succinate-*co*-lactate) (PBSL, the trade name: GS Pla®) was developed by Mitsubishi Chemical Corporation [18,19]. Although the conventional PBS manufactured by Showa Highpolymer Co., Ltd (trade name: Bionolle®) is chain-extended by hexamethylene diisocyante [20], the PBSL does not contain the isocyanate-based unit. The monomers for the synthesis of PBSL are succinic acid, 1,4-butanediol, and L-lactic acid, all of which can be derived from renewable plant-resources. Thus, succinic acid can be prepared by fermentation of starch, and the succinic acid can be converted to 1,4-butanediol by hydrogenation.

In this study, PBSL was blended with PLLA, and its mechanical properties, morphologies, and crystallization behaviors were investigated in comparison with those of

* Corresponding author. Tel.: +81 47 478 0423; fax: +81 47 478 0439.
E-mail address: shibata@sky.it-chiba.ac.jp (M. Shibata).

0032-3861/$ - see front matter © 2006 Elsevier Ltd. All rights reserved.
doi:10.1016/j.polymer.2006.03.065

PLLA/PBS blend. In particular, the present paper is focused on the improvement of the brittleness and low crystallization rate of PLLA without sacrificing the strength and modulus by blending a small amount of PBSL or PBS.

2. Experimental

2.1. Materials

PLLA (LACEA® H-100, melt flow rate (190 °C, 2.16 kg) 8 g/10 min, specific gravity 1.26) was supplied from Mitsui Chemicals Inc. (Japan). PBSL (GS Pla® AZ-type, lactate unit ca. 3 mol%, melt flow rate (190 °C, 2.16 kg) 25 g/10 min, specific gravity 1.26) was supplied from Mitsubishi Chemical Corporation (Japan). PBS (Bionolle® #1020, melt flow rate (190 °C, 2.16 kg) 25 g/10 min, specific gravity 1.26) was supplied from Showa Highpolymer Co. Ltd (Japan).

2.2. Sample preparation

The polymers were dried at 40 °C in a vacuum oven for at 24 h before use. Blending of PLLA and PBSL or PBS was performed using a Laboplasto-Mill with a twin rotary mixer (Toyo Seiki Co. Ltd, Japan). The molten mixing was carried out at 190 °C, the rotary speed was 50 rpm, and mixing time was 5 min. The obtained blends were cut into the small pieces and again dried at 40 °C in a vacuum oven before the injection molding. The weight ratios of PLLA/PBSL(PBS) were 100/0, 99/1, 95/5, 90/10, 80/20, 60/40, 40/60, 20/80 and 0/100. Dumbbell specimens (width 5 mm × thickness 2 mm × length of parallel part 32 mm × total length 72 mm) were molded using a desk injection molding machine (Little-Ace I Type, Tsubako Co. Ltd, Japan). The cylinder temperature and the molding temperature during the injection molding were 200 and 40 °C, respectively.

2.3. Measurements

Dynamic viscoelastic measurements were performed on a Rheolograph Solid (Toyo Seiki Co., Ltd, Japan) with a chuck distance of 20 mm, a frequency of 10 Hz and a heating rate of 2 °C /min.

The morphology of the blends was observed by field emission-scanning electron microscopy (FE-SEM), using a Hitachi S-4700 machine (Hitachi High-Technologies Corporation, Japan). All samples were fractured after immersion in liquid nitrogen for about 5 min. The fracture surfaces were sputter coated with gold to provide enhanced conductivity.

Tensile tests were performed using an Autograph AGS-500C (Shimadzu Co., Ltd, Japan) according to the standard method for testing the tensile properties of rigid plastics (JIS K7113 (1995)). Span length was 50 mm, and the testing speed was 10 mm/min. Five composite specimens were tested for each set of samples, and the mean values and standard deviation were calculated.

The differential scanning calorimetry (DSC) measurements were performed on a Perkin–Elmer DSC Pyris 1 DSC in a nitrogen atmosphere. First, the samples cut from the dumbbell-shaped blends were heated at a rate of 20 °C/min to evaluate the original crystallinity of the PLLA component of the blends. Next, non-isothermal crystallization behavior of the PLLA/PBSL(PBS) 95/5 blends after heated to 190 °C at a rate of 100 °C/min and held at that temperature for 3 min, was monitored at cooling rates of 1, 5, 20 °C/min. Also, in order to investigate the cold crystallization behavior of all the blends without the influence of thermal history, all the blends were heated to 190 °C at a rate of 100 °C/min, held at that temperature for 3 min, and then quenched at a cooling rate of 100 °C/min. After then, the second heating scans were monitored between 0 and 200 °C at a heating rate of 20 °C/min for determining glass transition temperature (T_g), cold crystallization temperature (T_c') and melting temperature (T_m). The T_g was obtained as the mid point of the heat capacity change. Next, in order to investigate the isothermal crystallization behavior of PLLA/PBSL(PBS) 100/0–90/10 blends, the blends were heated to 190 °C at a rate of 100 °C/min, held at this temperature for 3 min, and then cooled to 110 °C at a rate of 100 °C/min. The heat generated during the development of the crystalline phase was recorded at 110 °C until no further heat evolution was observed, and analyzed according to the usual procedure in order to obtain the relative degree of crystallinity. The relative degree of crystallinity as a function of time, was found from Eq. (1)

$$\frac{\chi_c(t)}{\chi_c(\infty)} = \frac{\int_{t_0}^{t} (dH/dt)dt}{\int_{t_0}^{\infty} (dH/dt)dt} \quad (1)$$

where t_0 is the time at which the sample attains isothermal conditions, as indicated by a flat baseline after the initial spike in the thermal curve, $\chi_c(t)$ is the degree of crystallinity at time t, $\chi_c(\infty)$ is the ultimate crystallinity at very long time, and dH/dt is the heat flow rate.

3. Results and discussion

3.1. Dynamic viscoelastic properties

Figs. 1 and 2 show dynamic viscoelastic curves of PLLA/PBSL and PLLA/PBS blends, respectively. The glass transition temperatures ($T_{g,PLLA}$, $T_{g,PBSL}$, and $T_{g,PBS}$) corresponding to PLLA, PBSL, and PBS components for the blends calculated from the tan δ peak temperature are summarized in Table 1. As is obvious from the tan δ curves, the PLLA/PBSL(PBS) blends containing PBSL(PBS) more than 10 wt% showed two glass transition temperatures ($T_{g,PLLA}$ and $T_{g,PBSL(PBS)}$). This result indicates that their blends are not miscible in the amorphous phase. The PLLA/PBSL(PBS) blends of PBSL(PBS) content from 1 to 10 wt% showed only one T_g corresponding to PLLA component, which slightly decreased with increasing PBSL(PBS) content. But this depression is largely deviated from the value expected from the classical Fox equation or the Gordon-Tayor equation, indicating that PBSL and PBS are

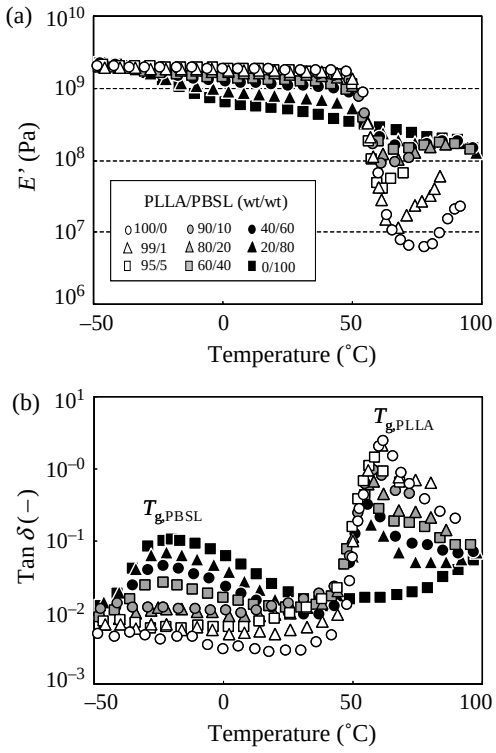

Fig. 1. Dynamic viscoelastic curves of PLLA/PBSL blends: (a) E' and (b) tan δ.

immiscible with PLLA, and their compatibility is not so good. Although PBSL contains lactate unit of ca. 3 mol%, there seems to be little difference in the compatibility with PLLA between PBSL and PBS. Among the PLLA/PBSL(PBS)

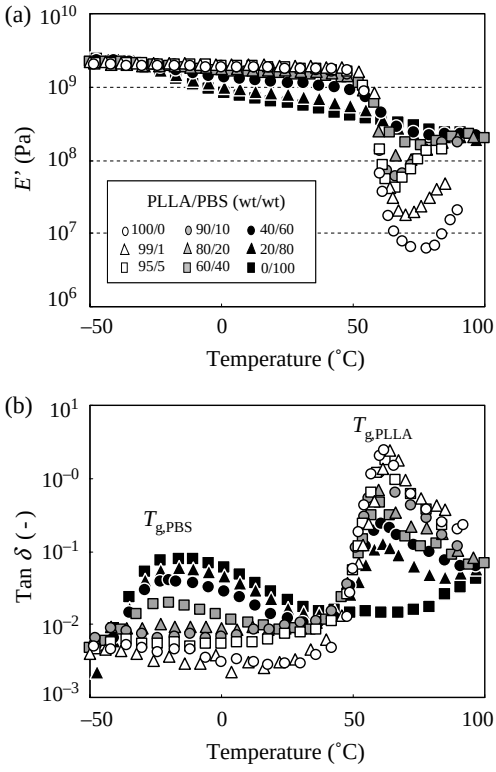

Fig. 2. Dynamic viscoelastic curves of PLLA/PBS blends: (a) E' and (b) tan δ.

Table 1
Glass transition temperatures measured by dynamic viscoelastic measurement for PLLA/PBSL and PLLA/PBS blends

PLLA/PBSL(PBS) weight ratio	PLLA/PBSL blends		PLLA/PBS blends	
	$T_{g,PBSL}$	$T_{g,PLLA}$	$T_{g,PBS}$	$T_{g,PLLA}$
100/0	–	62.1	–	62.1
99/1	–	61.1	–	64.2
95/5	–	58.4	–	62.2
90/10	–	58.1	–	60.1
80/20	−25.1	58.1	−23.0	59.9
60/40	−23.1	55.1	−21.0	59.0
40/60	−23.0	56.1	−20.0	60.2
20/80	−21.9	57.0	−20.0	60.9
0/100	−20.0	–	−15.9	61.1

blends, the PLLA/PBS 99/1 blend showed a exceptionally high $T_{g,PLLA}$. This result is discussed in the following section. Because the tan δ peak corresponding to $T_{g,PBSL(PBS)}$ is very broad, some errors for the peak maximum position should be considered. If PBSL(PBS) is compatible with PLLA, $T_{g,PBSL(PBS)}$ should increase with PLLA content. However, a little depression of $T_{g,PBSL(PBS)}$ with increasing PLLA content was observed for the PLLA/PBSL(PBS) 80/20–0/100 blends, indicating that PBSL(PBS) is immiscible with PLLA at least. The storage modulus (E') around 0–50 °C for PLLA/PBSL(PBS) blends gradually decreased with increasing amount of rubbery PBSL(PBS), as a whole. The E' of pure PLLA dropped around 50–60 °C due to glass transition, and then rose around 80 °C due to crystallization. The temperature where E' starts to increase due to crystallization of PLLA component shifted to a lower temperature region by addition of small amount of PBSL or PBS. This result suggests that the addition of PBSL or PBS enhances the cold crystallization of PLLA.

3.2. Morphologies by FE-SEM

Figs. 3 and 4 show the FE-SEM micrographs of PLLA/PBSL and PLLA/PBS blends, respectively. Although the phase separation was not confirmed by FE-SEM for the 99/1 blends, all the other blends appeared phase-separated, in agreement with the result of dynamic viscoelastic measurement. It appears that matrix phase is PLLA for the PLLA/PBSL(PBS) blends with PLLA content not less than 60 wt%, and phase inversion occurs for the corresponding 40/60–20/80 blends. As a whole, the dispersed phase was finely and homogeneously dispersed in the matrix for the blends with a low content of the dispersed component. The approximate diameters of the dispersed PBSL(PBS) phase were 0.1–0.4 μm at the PBSL(PBS) contents 5–20 wt%. The dispersed PLLA phase had a similar size for the blends with the PLLA content 20 wt%. The interface of PLLA and PBSL(PBS) is not so clear for some blends, indicating some compatibility of PLLA and PBSL(PBS).

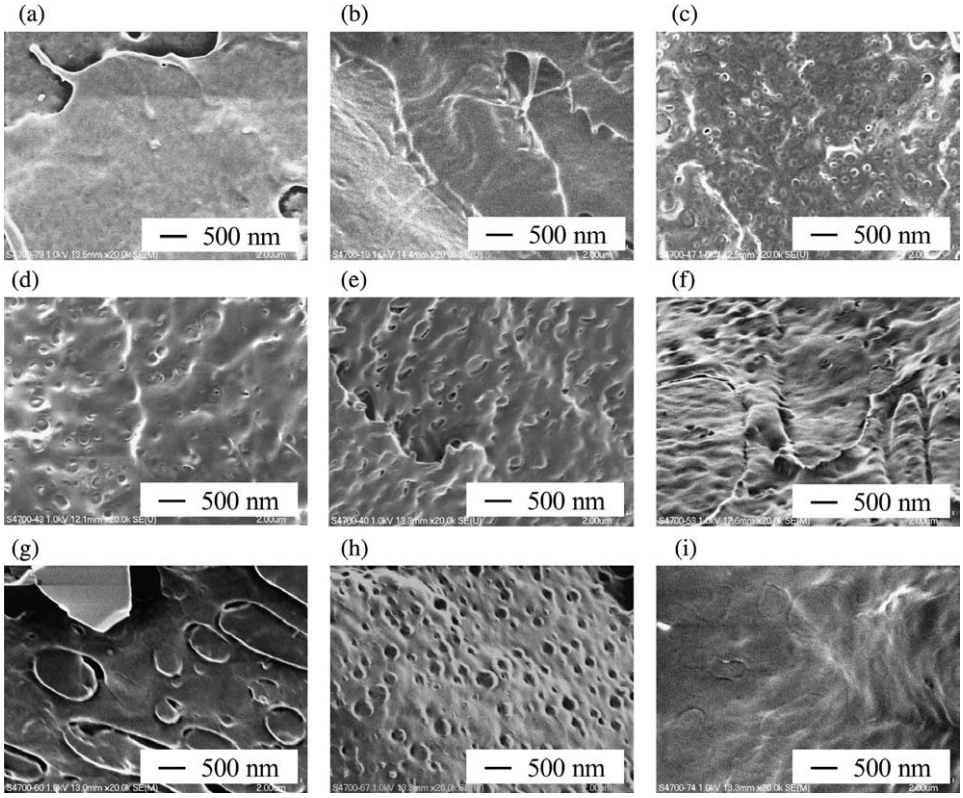

Fig. 3. FE-SEM images of PLLA/PBSL blends: PLLA/PBSL weight ratio (a) 100/0, (b) 99/1, (c) 95/5, (d) 90/10, (e) 80/20, (f) 60/40, (g) 40/60, (h) 20/80, and (i) 0/100.

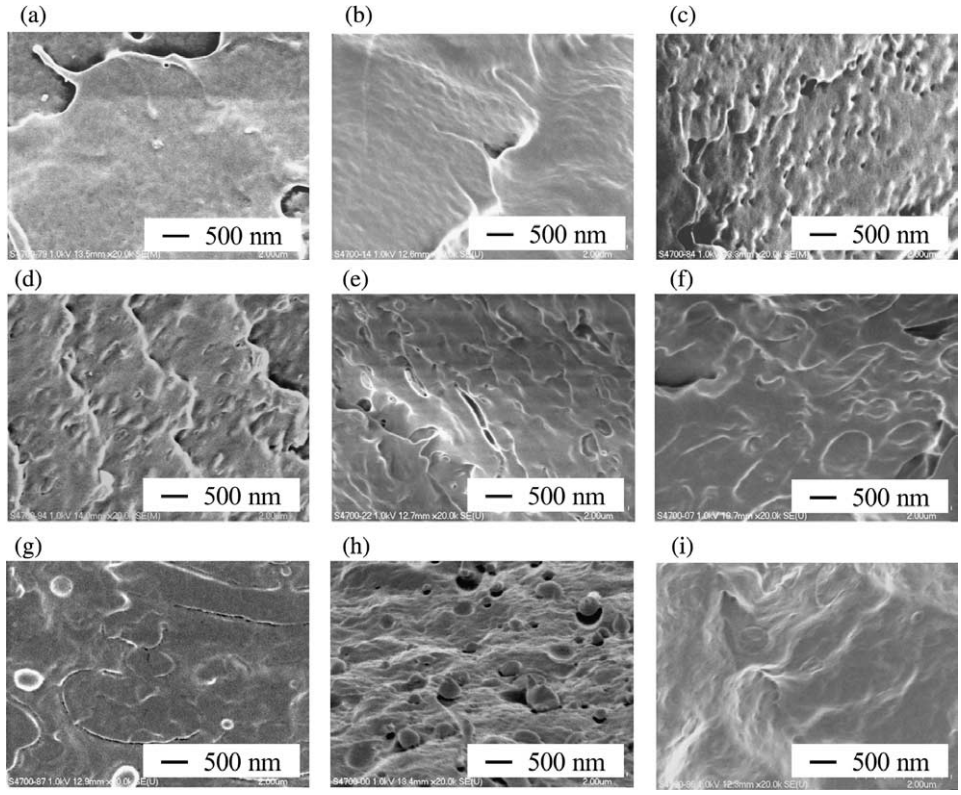

Fig. 4. FE-SEM images of PLLA/PBS blends: PLLA/PBS weight ratio (a) 100/0, (b) 99/1, (c) 95/5, (d) 90/10, (e) 80/20, (f) 60/40, (g) 40/60, (h) 20/80, and (i) 0/100.

3.3. Tensile properties

Fig. 5 shows the tensile properties of PLLA/PBSL and PLLA/PBS blends. The tensile strength and modulus of the PLLA/PBSL(PBS) blends approximately followed the rule of mixtures over the whole composition range except for the PLLA/PBS 99/1 and 95/5 blends. This result should be attributed to the formation of finely dispersed blends shown in Figs. 3 and 4. It is interesting that the PLLA/PBS 99/1 blend exceptionally shows higher tensile strength and modulus than pure PLLA. The PLLA/PBSL 99/1 blend did not show such a high tensile strength and modulus. The tan δ peak temperature (64.2 °C) of the PLLA/PBS 99/1 blend is considerably higher than that of PLLA/PBSL 99/1 blend (61.1 °C) or pure PLLA (62.1 °C) as is shown in Table 1, suggesting that PBS interacts with PLLA in the amorphous region of the blend. Although PBS has the urethane bond chain-extended by hexamethylene diisocyante, the main chain of PBSL is composed of only ester bond. We cannot specify the interaction between PBS and PLLA from these facts, but, it is thought that the polar urethane bond may interact with the terminal carboxylic acid or the main chain ester group of PLLA. Also, the PLLA/PBSL(PBS) blends showed much higher elongation at break than pure PLLA and pure PBSL(PBS) over the whole composition range (Fig. 5(c)). Typical stress–strain curves for pure PLLA and PLLA/PBSL(PBS) 95/5 and 90/10 blends are shown in Fig. 6. Although the yielding elongation at the maximum stress of the PLLA/PBSL blends is not so different from that of pure PLLA, the elongation at break is certainly improved by the addition of small amount of PBSL. Almost the similar trend was observed for the case of PLLA/PBS blends except that the PLLA/PBS 95/5 blend has exceptionally higher maximal stress than control PLLA. As a whole, PLLA/PBSL blends showed higher elongation at break and lower tensile strength and modulus than PLLA/PBS blends.

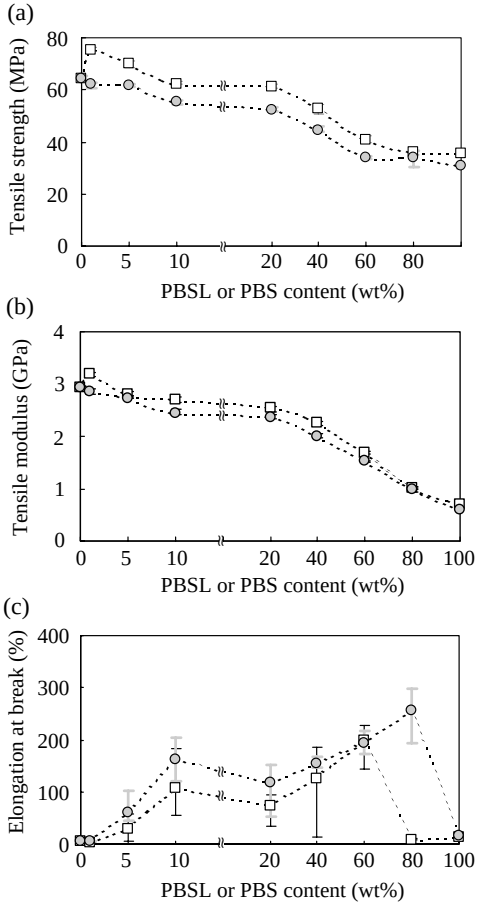

Fig. 5. Tensile properties of PLLA/PBSL (○) and PLLA/PBS (□) blends: (a) tensile strength, (b) tensile modulus, and (c) elongation at break.

3.4. Non-isothermal crystallization behavior by DSC

In order to investigate the factors for the exceptionally high tensile modulus of the PLLA/PBS 99/1–95/5 blends, it is necessary to compare the original degree of crystallinity of the PLLA component ($\chi_{c0,PPLA}$) for the dumbbell-shaped samples used for the tensile test. The $\chi_{c0,PPLA}$ was evaluated from the following equation

$$\chi_{c0,PPLA} = 100\frac{(\Delta H_{m,PLLA} - \Delta H'_{c,PLLA})}{(\Delta H^0_{m,PLLA} \cdot w_{PLLA})} \quad (2)$$

where $\Delta H_{m,PLLA}$ and $\Delta H'_{c,PLLA}$ are the heat of melting and cold crystallization of the injection-molded sample on the first heating DSC scan, respectively, ΔH^0_m is the heat of melting of 100% crystalline PLLA($\Delta H^0_m = 93$ J/g) [21], and w_{PLLA} is weight fraction of PLLA in the blend. The $\chi_{c0,PPLA}$'s of PLLA/PBS and PLLA/PBSL 99/1 blends are 5.5%, which is a little higher than that of pure PLLA, suggesting that the addition of PBSL(PBS) promotes the crystallization of the PLLA component, although we cannot strictly speak because the thermal history of the injection molded samples is not

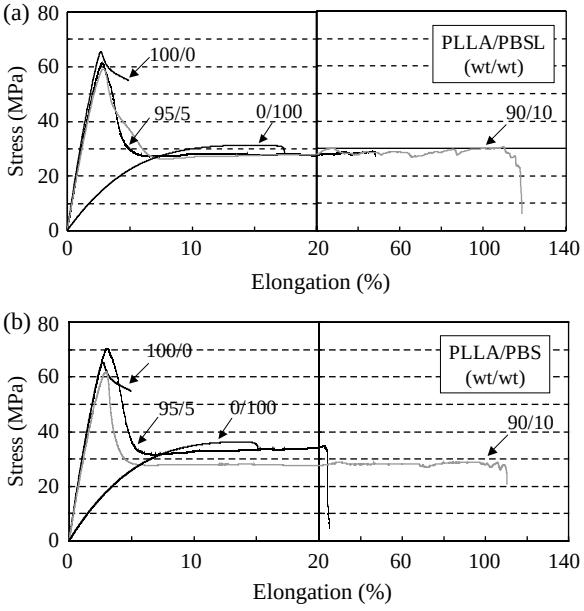

Fig. 6. Typical stress–strain curves for PLLA, PBSL, PBS, the PLLA/PBSL 95/5 and 90/10 blends, and the PLLA/PBS95/5 and 90/10 blends.

Table 2
DSC parameters obtained from the first heating scan for the PLLA/PBSL and PLLA/PBS (100/0–90/10) blend samples used for the tensile test

Blend	$T_{g,PLLA}$ (°C)	$T'_{c,PLLA}$ (°C)	$\Delta H'_{c,PLLA}$ (J/g)	$T_{m,PLLA}$ (°C)	$\Delta H_{m,PLLA}$ (J/g)	$\chi_{c0,PLLA}$ (%)
PLLA	60.7	124.0	24.3	161.8	27.8	3.8
PLLA/PBSL (99/1)	60.3	102.0	29.7	166.9	34.8	5.5
PLLA/PBSL (95/5)	61.5	90.2	29.9	166.4	35.1	5.6
PLLA/PBSL (90/10)	62.3	95.6	23.4	165.1	34.6	12.0
PLLA/PBS (99/1)	61.2	113.3	29.1	167.7	34.2	5.5
PLLA/PBS (95/5)	62.2	96.7	21.4	165.4	33.8	13.3
PLLA/PBS (90/10)	62.9	94.8	15.4	164.8	32.7	18.6

constant (Table 2). The reason why the PLLA/PBS 99/1 blend has higher tensile properties than PLLA/PBSL 99/1 and pure PLLA should not be attributed to the difference of crystallinity. As above mentioned, it is thought that some interaction between PBS and PLLA in the amorphous region contributes.

Next, non-isothermal crystallization behavior of the PLLA component at a cooling stage from the melted state of the PLLA/PBSL and PLLA/PBS 95/5 blends at 190 °C was monitored by DSC. Fig. 7 shows their cooling thermograms at cooling rates of 1, 5, and 20 °C/min in comparison with those of PLLA. All the samples showed no exothermic peak due to the crystallization of the PLLA component at a cooling rate of 20 °C/min. When a cooling rate is 5 °C/min, the PLLA crystallization similarly did not occur for PLLA and the PLLA/PBS 95/5 blend. However, the PLLA/PBSL 95/5 blend showed an exothermic peak at 100.2 °C ($\Delta H_{c,PLLA}$: 13.8 J/g-PLLA), indicating that the crystallization of the PLLA component is promoted by the addition of PBSL. When a cooling rate is 1 °C/min, the PLLA crystallization occurred for all the samples. In this case, although there was little difference in $T_{c,PLLA}$ and $\Delta H_{c,PLLA}$ between PLLA and the PLLA/PBS 95/5 blend, the PLLA/PBSL 95/5 blend showed considerably higher $T_{c,PLLA}$ and $\Delta H_{c,PLLA}$. It is very interesting that the crystallization of PLLA at a cooling stage is enhanced by the addition of a small amount of PBSL, while PBS is not effective.

Next, the cold crystallization behavior of all the blends at the second heating stage was investigated using the samples quenched at a cooling rate of 100 °C/min after melted at 190 °C for 3 min. On this cooling stage, no exothermic peak due to crystallization of the PLLA component was observed, while the crystallization of the PBSL(PBS) component occurred. Fig. 8 shows the second heating scan for PLLA/PBSL(PBS) blends at a rate of 20 °C/min. Table 3 summarizes the DSC parameters obtained from this heating run. The cold crystallization temperature for PLLA component ($T'_{c,PLLA}$) shifted to a lower temperature region, and its enthalpy $\Delta H'_{c,PLLA}$ increased by addition of small amount of PBSL (1 and 5 wt%), indicating that the addition of PBSL enhances the cold crystallization of PLLA component. The addition of PBSL more than 5 wt% does not cause a further crystallization enhancement, judging from the values of $T'_{c,PLLA}$ and $\Delta H'_{c,PLLA}$ of the PLLA/PBSL 90/10 and 80/20 blends. Regarding the PLLA/PBSL 60/40–20/80 blends, we could not strictly evaluate the change of DSC parameters, because the exothermic peaks due to crystallization of PLLA and PBSL overlapped with the endothermic

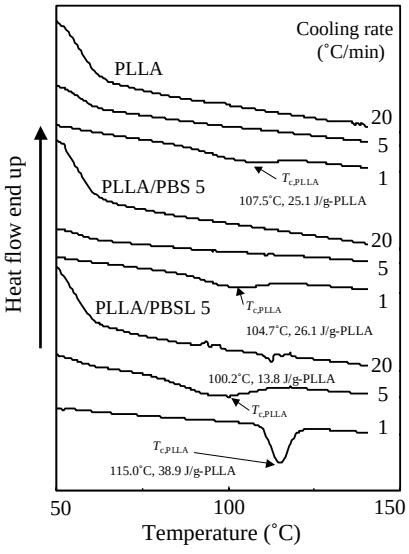

Fig. 7. The cooling DSC thermograms at a cooling rate of 1, 5, and 20 °C/min for PLLA, PLLA/PBS 95/5 blend, and PLLA/PBSL 95/5 blend melted at 190 °C for 3 min.

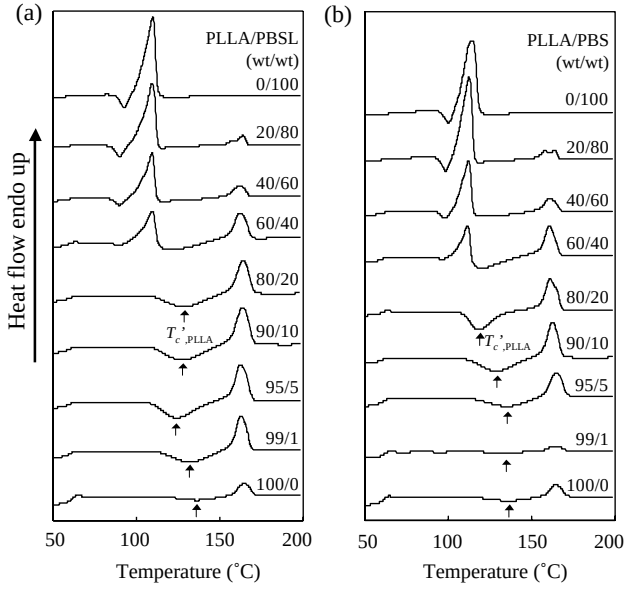

Fig. 8. The second heating DSC thermograms at a heating rate of 20 °C/min for (a) PLLA/PBSL blends and (b) PLLA/PBS blends quenched at a cooling rate of 100 °C/min after melted at 190 °C for 3 min.

Table 3
DSC parameters obtained from the second heating scan for PLLA/PBSL and PLLA/PBS blends after quenched at a cooling rate of 100 °C/min from the melt

Blend	PLLA component					PBSL(PBS) component			
	T_g (°C)	T_c' (°C)	$\Delta H_c'$ (J/g)	T_m (°C)	ΔH_m (J/g)	T_c' (°C)	$\Delta H_c'$ (J/g)	T_m (°C)	ΔH_m (J/g)
PLLA	60.5	136.3	6.38	164.5	7.02	–	–	–	–
PLLA/PBSL (99/1)	59.4	132.0	23.1	162.8	25.3	–	–	–	–
PLLA/PBSL (95/5)	58.2	124.2	33.2	162.4	38.1	–	–	–	–
PLLA/PBSL (90/10)	58.1	127.3	28.4	163.8	31.6	–	–	–	–
PLLA/PBSL (80/20)	59.0	128.3	29.6	164.1	30.9	–	–	–	–
PLLA/PBSL (60/40)	58.5	120.9[a]	25.2[a]	162.1	32.2	89.3[a]	4.7[a]	109.5[a]	44.3[a]
PLLA/PBSL (40/60)	57.4	116.2[a]	15.8[a]	161.8	28.0	89.7[a]	7.5[a]	109.1[a]	59.5[a]
PLLA/PBSL (20/80)	57.0	115.6[a]	20.6[a]	157.4/ 163.8	32.3	89.7[a]	7.4[a]	109.5[a]	56.9[a]
PBSL	–	–	–	–	–	92.7	8.0	109.8	58.3
PLLA/PBS (99/1)	60.6	133.9	2.53	164.0	4.56	–	–	–	–
PLLA/PBS (95/5)	59.9	135.6	14.9	164.8	16.6	–	–	–	–
PLLA/PBS (90/10)	58.2	128.9	30.6	162.8	33.4	–	–	–	–
PLLA/PBS (80/20)	58.7	118.2	35.6	161.1	39.9	–	–	–	–
PLLA/PBS (60/40)	58.6	120.2[a]	27.5[a]	160.7	37.7	96.4[a]	1.5[a]	111.5[a]	45.8[a]
PLLA/PBS (40/60)	58.2	119.2[a]	27.5[a]	160.9	26.5	98.1[a]	6.2[a]	112.1[a]	50.3
PLLA/PBS (20/80)	56.9	118.5[a]	24.5[a]	157.6/ 163.7	35.0	98.4[a]	6.8[a]	112.5[a]	53.6
PBS	–	–	–	–	–	100.1	5.8	114.5	59.9

[a] The separation of the exothermic peaks due to cold crystallization of PLLA and PBSL(PBS) components and the endothermic peak due to melting of PBSL(PBS) is not sufficient.

peak due to melting of PBSL, as is shown in Fig. 8. The addition of PBS enhanced the cold crystallization of PLLA component in a similar manner as the case of PBSL. However, the crystallization enhancement of the PLLA/PBS 99/1–95/5 blends is much less than that of the PLLA/PBSL 99/1–95/5 blends, as is obvious from the values of $\Delta H'_{c,PLLA}$ and $\Delta H_{m,PLLA}$ (Table 3). This result may relate to a special interaction between PLLA and PBS in the amorphous region mentioned above. The $T_{g,PLLA}$ (60.6 °C) measured by DSC for PLLA/PBS 99/1 blend is also a little higher than that (59.4 °C) of PLLA/PBSL 99/1 blend, in agreement with the result of dynamic viscoelastic measurement. It is thought that the mobility of PLLA chain affects the difference of the crystallization.

3.5. Isothermal crystallization behavior by DSC

The isothermal crystallization behavior of the PLLA component was monitored at 110 °C by DSC after the PLLA/PBSL(PBS) (100/0–90/10) blends were melted at 190 °C for 3 min. The isothermal crystallization kinetic of the blend was analyzed by means of Avrami equation

$$\frac{\chi_c(t)}{\chi_c(\infty)} = 1 - \exp(-kt^n) \quad (3)$$

where k is the rate constant of crystallization and n is the Avrami exponent, which can be related to the type of nucleation and to the geometry of crystal growth. From the intercepts and the slopes of the plots of $\log[-\ln(1-\chi_c(t)/\chi_c(\infty))]$ versus $\log t$ (Fig. 9), the values of k and n were calculated, respectively; all these values are summarized in Table 4. As each curve has a linear portion followed by a gentle roll-off at longer times, the slope at the shorter crystallization time corresponding primary crystallization was adopted. The obtained n for pure PLLA was 2.6, which should be three-dimensional crystal growth assuming heterogeneous nucleation. Some nuclei of PLLA are thought to remain at the melting at 190 °C for 3 min. Miyata et al. reported that n value is ca. 4 for isothermal crystallization at 90–140 °C after melted at 200 °C for 10 min [22]. This case is assigned to three-dimensional growth with a homogeneous nucleation mode. We did not adopt this melting condition because some decomposition of PBSL or PBS component at 200 °C is thought. The crystallization half-time ($t_{1/2}$), the time at which the relative degree of crystallization is 0.5, significantly decreased with increasing PBSL content. In contrast to this result, little shortening of $t_{1/2}$ was observed for the PLLA/PBS blends. Also, the rate constant of the PLLA/PBSL blends was much higher than that of the PLLA/PBS blends. It is interesting that PBSL significantly enhances the isothermal crystallization of PLLA, while the addition of PBS is ineffective.

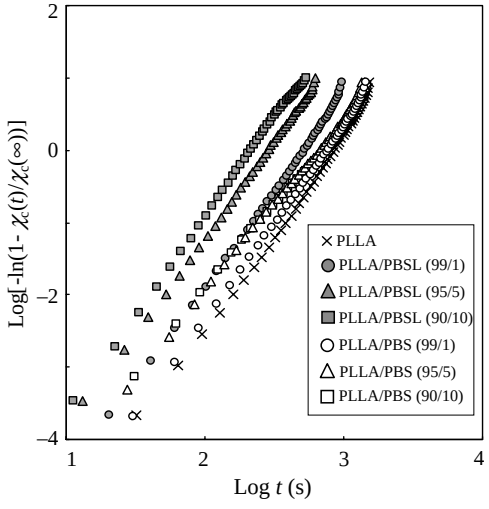

Fig. 9. $\log[-\ln(1-\chi_c(t)/\chi_c(\infty))]$ versus $\log t$ for the PLLA/PBSL and PLLA/PBS blends at T_c 110 °C.

Table 4
Isothermal crystallization parameters at 110 °C for the PLLA in the blends with PBSL and PBS

Blend	Weight ratio	$t_{1/2}$ (min)	K (s^{-n})	n	$\chi_{c,PLLA}$ (%)
PLLA	100	12.5	2.47×10^{-8}	2.59	42.6
PLLA/PBSL	99/1	8.43	5.38×10^{-8}	2.67	38.1
PLLA/PBSL	95/5	4.15	2.48×10^{-7}	2.69	41.4
PLLA/PBSL	90/10	3.12	2.86×10^{-7}	2.81	45.2
PLLA/PBS	99/1	11.2	2.07×10^{-8}	2.66	40.3
PLLA/PBS	95/5	9.59	1.20×10^{-7}	2.45	40.5
PLLA/PBS	90/10	10.35	1.77×10^{-7}	2.36	39.1

The normalized degree of crystallinity ($\chi_{c,PLLA}$) of the isothermally crystallized blend was estimated from the DSC results by using the following equation

$$\chi_{c,PLLA} = 100\Delta H_c/(\Delta H^0_{m,PLLA}\cdot w_{PLLA}) \quad (4)$$

where ΔH_c is the total heat of the isothermal crystallization. The PLLA/PBSL(PBS) blends (38–45%) had a comparable $\chi_{c,PLLA}$ to pure PLLA (42.6%). Therefore, it can be said that the crystallinity comparable to pure PLLA is obtained by the isothermal crystallization for a considerably shorter time in case of the PLLA/PBSL blends containing 1–5 wt% PBSL.

4. Conclusions

The PLLA blends with various compositions of PBSL and PBS were prepared by melt-mixing and subsequent injection molding, and their mechanical properties, morphology, and crystallization behavior were compared. Dynamic viscoelasticity and FE-SEM measurements revealed that the PLLA/PBSL(PBS) blends are finely dispersed immiscible blends, and the structure difference between PBSL and PBS had little influence on the compatibility with PLLA. The tensile strength and modulus of the blends approximately followed the rule of mixtures over the whole composition range except that those of PLLA/PBS 99/1 blend were exceptionally higher than those of pure PLLA. All the blends showed considerably higher elongation at break than pure PLLA, PBSL, and PBS. DSC analyses of the blends revealed that the addition of a small amount of PBSL enhances both the isothermal and non-isothermal PLLA crystallization from the melted state and the non-isothermal cold crystallization from the glassy state, while the addition of PBS is much less effective. Especially, the crystallization enhancement during a cooling stage is very important on an actual injection or extrusion molding. The PLLA/PBSL 99/1–90/10 blends are promising materials having better flexibility and higher crystallization rate than pure PLLA. In addition, it is interesting that the PLLA/PBS 99/1 blend has higher tensile strength and modulus than pure PLLA.

References

[1] Garlotta D. J Polym Environ 2001;9(2):63–84.
[2] Fujimaki T. Polym Degrad Stab 1998;59:209.
[3] Stärke D, Skupin G. Kunststoffe 2001;91(9):KU100.
[4] Marshall D. Eur Plast News 1998;25(3):23–4 see also p. 26.
[5] Goldberg D. J Environ Polym Degrad 1995;3(2):61–7.
[6] Ritter SK. Chem Eng News 2002;80(47):19–23.
[7] Smith C. Eur Plast News 2004;31(9):17–18.
[8] Vink ETH, Rabago KR, Glassner DA, Gruber PR. Polym Degrad Stab 2003;80(3):403–19.
[9] Sawyer DJ. Macromol Symp 2003;(201):271–81.
[10] Kim JK, Park DJ, Lee MS, Ihn KJ. Polymer 2001;42(17):7429–41.
[11] Martin O, Averous L. Polymer 2001;42(14):6209–19.
[12] Urayama H, Kanamori T, Fukushima K, Kimura Y. Polymer 2003;44(19):5635–41.
[13] Takagi J, Nemoto T, Takahashi T, Taniguchi T, Koyama K. Seikei-Kakou 2003;15(8):581–7.
[14] Park JW, Im SS. J Appl Polym Sci 2002;86:647–55.
[15] Yang JM, Chen HL, You JW, Hwang JC. Polym J 1997;29:657–62.
[16] Tsuji H, Ikada Y. J Appl Polym Sci 1998;67(3):405–15.
[17] Tamura N, Chitose T, Komai K, Takahasi S, Kssemura T, Obuchi S. Trans Mater Res Soc Jpn 2004;29(5):2017–20.
[18] Tukahara T. JETI 2004;52(13):119–21.
[19] Kishimoto M, Yamagishi K, Ueda T. JETI 2004;52(4):171–3.
[20] Ray SS, Okamoto K, Okamoto M. Macromolecules 2003;36:2355–67.
[21] Fisher EW, Sterzel HJ, Wegner G. Kolloid ZZ Polym 1973;251:980.
[22] Miyata T, Masuko T. Polymer 1998;39(22):5515–21.